Journal of Organometallic Chemistry, 355 (1988) 533–550
Elsevier Sequoia S.A., Lausanne – Printed in The Netherlands

Synthesis and reactivity of mixed-metal Pd_2Mo, PdPtMo and Pd_2W clusters containing $Ph_2PCH_2PPh_2$(dppm) ligands. Molecular structure of $[Pd_2MoCl(\eta\text{-}C_5H_5)(\mu_3\text{-}CO)_2(\mu\text{-dppm})_2]$ *

Pierre Braunstein, Michel Ries, Claude de Méric de Bellefon,

Laboratoire de Chimie de Coordination, associé au CNRS (UA 416), Université Louis Pasteur 4, rue Blaise Pascal, F-67070 Strasbourg Cedex (France)

Yves Dusausoy and Jean-Paul Mangeot

Laboratoire de Minéralogie et Cristallographie, associé au CNRS (UA 809), Université de Nancy I, Boîte postale 239, F-54506 Vandoeuvre-les-Nancy Cedex (France)

(Received April 18th, 1988)

Abstract

The quantitative synthesis of the heterotrinuclear chlorocarbonyl clusters $[PdM^1MCpCl(CO)_2(\mu\text{-dppm})_2]$ ($Cp = \eta\text{-}C_5H_5$, dppm = $Ph_2PCH_2PPh_2$, M^1 = Pd, M = Mo, **1**; M^1 = Pd, M = W, **2**; M^1 = Pt, M = Mo, **3**) was achieved by the reaction of $[M(CO)_3Cp]^-$ (M = Mo, W) with the dinuclear d^9–d^9 complexes $[PdM^1Cl_2(\mu\text{-dppm})_2]$ (M^1 = Pd, Pt) in THF. These clusters are characterized by a triangular metal core, whose Pd–M^1 and M^1–M edges are bridged by a dppm ligand. The two carbonyl ligands attached to M interact in a triply semi-bridging fashion with the three metals, on either side of the trimetallic plane. The chloride atom is always bonded to the trimetallic core PdM^1M via the Pd atom. This was established by an X-ray diffraction study on **1**: triclinic, space group $P\bar{1}(C_i^1)$, with $Z = 2$, a 13.664(2), b 13.946(5), c 18.223(6) Å, α 110.30(3), β 93.89(2), γ 102.22(2)°, V 3144.3(1) Å^3. The number of data used was 5675 (with $I > 5\ \sigma(I)$), giving values of $R = 0.046$ and $R_w = 0.046$ after refinement. In the presence of $Tl[PF_6]$, clusters **1** and **2** react with CO to give the cationic clusters $[Pd_2MCp(CO)(\mu\text{-}CO)_2(\mu\text{-dppm})_2]^+$ (M = Mo, $[\mathbf{4}]^+$; M = W, $[\mathbf{5}]^+$) which possess a CO ligand terminally bound to Pd, or with THF to give the solvento clusters $[Pd_2MCp(CO)_2(THF)(\mu\text{-dppm})_2]^+$ (M = Mo, $[\mathbf{7}]^+$; M = W, $[\mathbf{8}]^+$). The heterotetranuclear metalloligated clusters $[PdM^1M_2Cp_2(CO)_5(\mu\text{-dppm})_2]$ (M^1 = Pd, M = Mo, **9**; M^1 = Pd, M = W, **10**; M^1 = Pt, M = Mo, **11**) have

* Dedicated to Professor E.O. Fischer on the occasion of his 70 birthday, with our sincere congratulations.

0022-328X/88/$03.50

been prepared from **1–3**, respectively. Their relevance to the mechanism of formation of clusters **1–3** is discussed, particularly in view of the lability of their exocyclic, equatorial Pd–M bond.

Introduction

We have shown previously that the complexes $[PdM^1Cl_2(\mu\text{-dppm})_2]$ (M^1 = Pd, Pt; dppm = $Ph_2PCH_2PPh_2$) react with the carbonylmetalates $[Co(CO)_4]^-$, $[Fe(CO)_3NO]^-$ or $[Mn(CO)_5]^-$ to afford tetranuclear clusters having planar cores of composition PdM^1Co_2, PdM^1Fe_2 or PdM^1Mn_2. They consist of a metal triangle bridged by two dppm ligands and bound to an equatorial, metalloligated fragment [1]. A unique structural feature of these clusters is the presence of the bridging $[M^2]$ fragment whose bonding has been discussed and compared with that of 18-electron carbonylmetalates in other *closo*-structures [1d–f].

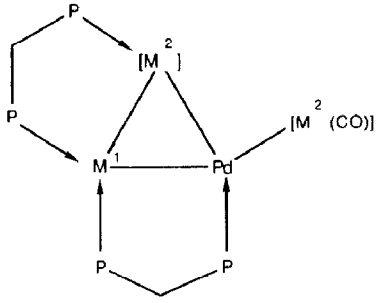

M^1 = Pd, Pt

$[M^2]$ = $Mn(CO)_4$, $Fe(CO)_2NO$, $Co(CO)_3$

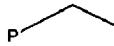

= $Ph_2PCH_2PPh_2$ (dppm)

Studies have shown, e.g., that these syntheses are regioselective owing to the greater lability of the Pd–P vs. Pt–P bond in the precursor, and that the most reactive site in these clusters is the exocyclic palladium–transition metal bond. In order to evaluate further the influence of the metal carbonyl precursor on the synthesis, structure and properties of such clusters, we have investigated the reaction of $[PdM^1Cl_2(\mu\text{-dppm})_2]$ with the group 6 carbonylmetalates $[Mo(CO)_3Cp]^-$ and $[W(CO)_3Cp]^-$ ($Cp = \eta\text{-}C_5H_5$). Trinuclear clusters having a chloride atom bound to palladium in place of the metalloligand were isolated instead, as reported in the preliminary communication [1a], and as now confirmed by an X-ray diffraction study. They are easily converted into cationic clusters by reaction with a halide abstractor in the presence of carbon monoxide.

Results and discussion

The reaction of $[PdM^1Cl_2(\mu\text{-dppm})_2]$ with one equiv of the anions $[M(CO)_3Cp]^-$ (M = Mo or W), in refluxing THF, gave red-brown solutions from which the new trinuclear clusters $[PdM^1MCpCl(CO)_2(\mu\text{-dppm})_2]$ (M^1 = Pd, M = Mo, **1**; M^1 = Pd, M = W, **2**; M^1 = Pt, M = Mo, **3**) were obtained in quantitative yields (eq. 1). When two equiv of $[M(CO)_3Cp]^-$ were used, only these trinuclear clusters were formed (IR and $^{31}P\{^1H\}$ NMR evidence). Details of the formation of **1** or **2** are given below.

The IR spectrum of **1–3** shows a strong and a weaker ν(CO) absorption band near 1755 and 1795 cm^{-1}, respectively (Table 1). This is consistent with the symmetric and antisymmetric vibration modes of a $M(CO)_2$ moiety whose carbonyl

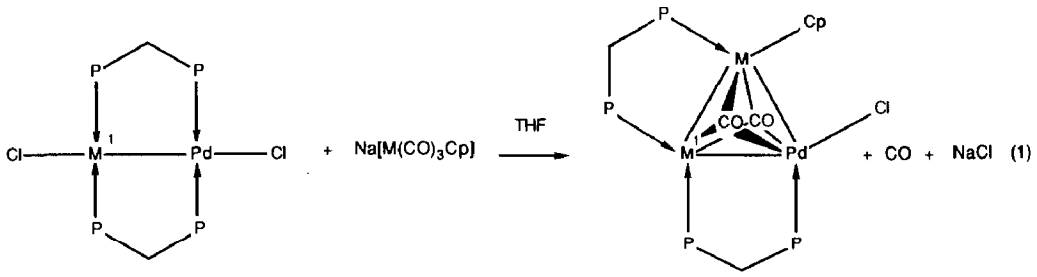

1, M^1 = Pd, M = Mo

2, M^1 = Pd, M = W

3, M^1 = Pt, M = Mo

ligands are bent over the triangular core in a triply semi-bridging fashion, as also shown by the molecular structure of **1** determined by X-ray diffraction (see below). Their FIR spectrum shows a ν(Pd–Cl) vibration around 257 cm^{-1}. In the ^1H NMR spectrum (see Table 2) the signals due to the methylenic protons of the dppm ligands present a pattern typical of the triangulo unit bridged by two dppm ligands which has been previously discussed [1e,f]. In the case of **2**, only a disymmetric triplet is seen due to accidental overlap of the two signals. The $^{31}P\{^1H\}$ NMR spectrum of **1** and **2** shows clearly one phosphorus atom bonded to Mo ($\delta \approx 49$ ppm) or W ($\delta \approx 17$ ppm, ^{183}W satellites) (see Table 3 and Fig. 1).

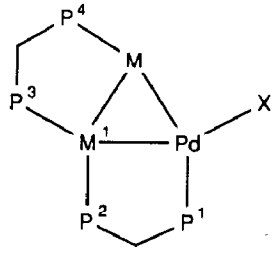

Table 1

Infrared spectral data

Complex	IR abs. max. ν(CO) [a] (cm^{-1})	
	Solid state [b]	Solution [c]
$[Pd_2MoCpCl(CO)_2(dppm)_2]$ (**1**)	1797w, 1756s	1750s
$[Pd_2WCpCl(CO)_2(dppm)_2]$ (**2**)	1793w, 1752s	1748s
$[PdPtMoCpCl(CO)_2(dppm)_2]$ (**3**)	1794w, 1749s	1796w, 1751s
$[Pd_2MoCp(CO)_3(dppm)_2][PF_6]$ (**4**[PF_6])	2036s, 1790s, br	2039s, 1786s, br
$[Pd_2WCp(CO)_3(dppm)_2][PF_6]$ (**[5]**[PF_6])	2040s, 1770s, br	2036s, 1783s, br
$[Pd_2WCpBr(CO)_2(dppm)_2]$ (**6**)	1790w, 1750s	–
$[Pd_2Mo_2Cp_2(CO)_5(dppm)_2]$ [d] (**9**)	–	1942w, 1892m, 1857w, 1815s, 1805s, 1749w
$[Pd_2W_2Cp_2(CO)_5(dppm)_2]$ [d] (**10**)	–	1945w, 1890m, 1860w, 1805s, br, 1745w

[a] Abbreviations: s = strong, m = medium, w = weak, br = broad. [b] Recorded as KBr pellet. [c] Recorded in THF. [d] Recorded in toluene.

Table 2

^{1}H NMR data [a]

Complex	C_5H_5 [b]		P-CH_2-P [c]			P-CH_2-P [c]	
	δ	^3J(PH)	δ	^2J(PH)	^4J(PH)	δ	^2J(PH)
$[Pd_2MoCpCl(CO)_2(dppm)_2]$ (1)	4.84 (d)	1.1	4.19 (dt)	9.0	ca. 2	3.99 (t)	9.8
$[Pd_2WCpCl(CO)_2(dppm)_2]$ (2)	4.90 (d)	1.2	4.29 (m) [d]	[e]	[e]	[e]	[e]
[PdPtMoCpCl$(CO)_2$(dppm)$_2$] [f] (3)	4.91 (dd)	0.9, 2.2	4.50 (ddd)	10.8, 7.9	2.1	4.27 (t)	10.2
$[Pd_2MoCp(CO)_3(dppm)_2][PF_6]$ ([4][PF_6])	4.90 (d)	2.4	4.54 (dt)	8.7	ca. 2	4.18 (t)	10.1
$[Pd_2WCp(CO)_3(dppm)_2][PF_6]$ ([5][PF_6])	4.97 (d)	2.3	4.62 (dt)	9.6	ca. 2	4.49 (t)	10.1
$[Pd_2WCpBr(CO)_2(dppm)_2]$ (6)	4.87 (d)	1.0	4.38 (m) [d]	[e]	[e]	[e]	[e]

[a] Recorded in $CDCl_3$ otherwise stated; (δ in ppm; J in Hz); d = doublet, m = multiplet, t = triplet. All compounds exhibit a complex multiplet in the range 7.7 to 6.7 (40 H) due to the phenyl groups of the dppm ligands. [b] Integration: 5H. [c] Integration: 2H. [d] Center of the multiplet (4H) arising from accidental overlap of the signals of both methylene groups. [e] Not determined, see [d]. [f] Recorded in CD_2Cl_2. ^3J(PtH) 62 Hz (respectively 39 Hz) for methylene at 4.50 ppm (respectively 4.27 ppm).

The three phosphorus atoms bonded to palladium have resonances in the range $\delta = -4$ to -11 ppm for **1** and -10 to -18 ppm for **2**. In order to help with the assignment of these three resonances, cluster [PdPtMoCpCl$(CO)_2(\mu$-dppm$)_2$] (**3**) was synthesized, in the same way as **1** (eq. 1). Thus in **3**, the phosphorus atoms P(2) and P(3) are coordinated to platinum (^1J(Pt–P) = 3232 and 3735 Hz, respectively), and P(1), being attached to palladium, is therefore unambiguously assigned [1e,f]. However, the assignments of P(2) and P(3) are mainly based on the J(PP) values previously encountered, but we cannot rule out the possibility that they should be interchanged. It is noteworthy that the ^3J[P(1)–P(4)] values for these clusters are much smaller than those for the analogous Mn-, Fe-, or Co-containing clusters, in which they range from ca. 60 to 140 Hz [1e,f].

Reactivity studies

The reaction of **1** or **2** with CO in the presence of a stoichiometric amount of Tl[PF_6] leads to quantitative formation of the cationic clusters [**4**][PF_6] or [**5**][PF_6] (eq. 2), respectively.

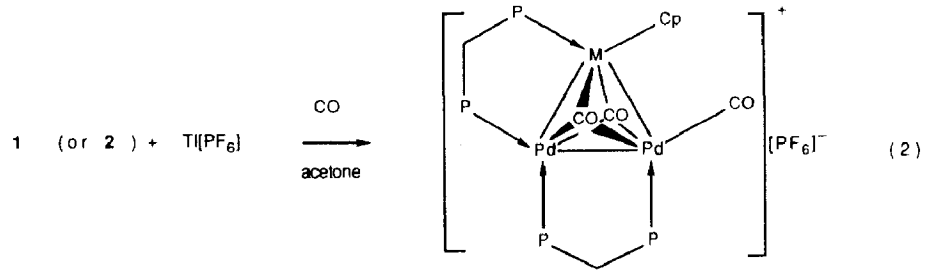

(2)

[4]$^+$, M = Mo

[5]$^+$, M = W

Compared with those of their neutral precursors, the IR spectrum of both clusters $[4]^+$ and $[5]^+$ exhibits a new ν(CO) band at ca. 2040 cm^{-1}, which is attributed to the carbonyl ligand terminally bound to palladium. The other strong ν(CO) band is shifted to higher wavenumbers, consistent with the cationic nature of these clusters (Table 1). Their ^1H NMR spectra present the typical pattern (a doublet of triplet and a triplet) for the methylenic protons of the dppm ligands. These two signals are shifted downfield compared with those from the parent neutral molecules **1** and **2**. The ^{31}P $\{^1H\}$ NMR spectra of $[4]^+$ and $[5]^+$ exhibit four well separated sets of signal. Their assignment has been made according to the criteria previously noted for **1** and **2**. The main feature of both spectra appears to be a strong downfield shift of P(2) when compared with the value for **1** or **2**.

The terminal carbonyl ligand of $[4]^+$ of $[5]^+$ is bound to the Pd atom sufficiently strongly that it cannot be removed by purging their THF solutions under vacuum. This contrasts with the behavior of related dppm clusters with Pd_2Co or Pd_2Fe cores, which can be readily decarbonylated under such conditions [1e,f]. However, CO is displaced by MeCN, which may be further replaced e.g., by Br^-, as also observed during the preparation of KBr pellets (IR evidence). The strengthening of this Pd–CO bond is consistent with its lower ν(CO) frequency (ca. 2040 cm^{-1}) compared with that found for the more labile $[Pd_2Co(CO)_4(\mu\text{-dppm})_2]^+$ analogue (2072 cm^{-1}) [1d].

Cluster $[Pd_2WCpBr(CO)_2(\mu\text{-dppm})_2]$ (**6**) was obtained in good yield, either by the metathesis involving exchange of Cl^- in **2** for Br^- or by the reaction of Br^- with the cationic cluster $[5]^+$ (eq. 3). Cluster **6** presents spectroscopic features (IR, ^1H and ^{31}P $\{^1H\}$ NMR, see Tables) very similar to those for **2**.

$[Pd_2WClCp(CO)_2(dppm)_2]$ (2)

or

$[Pd_2WCp(CO)_3(dppm)_2][PF_6]$ ($[5][PF_6]$)

$\xrightarrow{+\ Br^-}$

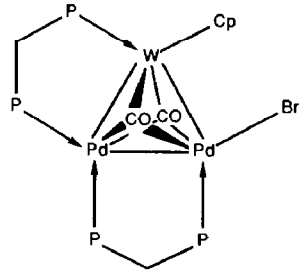

6

(3)

In order to evaluate further the stability and reactivity of these new Pd–Mo and Pd–W clusters, various reactions were attempted. Only unchanged **2** was recovered after treatment with MeLi or KO-t-Bu, known to be strong bases, able, e.g., to deprotonate the dppm ligand [2]. However, the reaction of MeLi with $[5][PF_6]$, carried out under CO, was immediate, even at low temperature, and led to fragmentation of the cluster, although some $[5]^+$ was reformed during work-up. A fragmentation product of $[5]^+$ exhibited in ^{31}P $\{^1H\}$ NMR a singlet at 11 ppm, which was previously encountered when $[Pd_2Fe(CO)_4(\mu\text{-dppm})_2]$ [3a] was treated with CO, confirming that it contains only palladium as a metal [3b]. The reaction of **2** with $HgCl_2$ led to fragmentation of the cluster and formation of $[PdCl_2(dppm)]$, the $HgCl_2$ acting as an oxidizing agent towards Pd^I. We also observed this behaviour when the Pd^I dinuclear complex $[Pd_2Cl_2(\mu\text{-dppm})_2]$ was treated with $HgCl_2$.

A striking feature of eq. 1 is the isolation of heterotrinuclear clusters bearing a

Table 3

^{31}P {^{1}H} NMR data [a]

Complex	δ [b]				J(P–P)						J(W–P(4))
	δ_1	δ_2	δ_3	δ_4	J(1–2)	J(1–3)	J(1–4)	J(2–3)	J(2–4)	J(3–4)	
$[Pd_2MoCpCl(CO)_2(dppm)_2]$ (**1**)	−6.1	−10.5	−4.2	48.8	76	40	20	43	77	25	
$[Pd_2WCpCl(CO)_2(dppm)_2]$ (**2**)	−17.4	−12.9	−10.6	17.0	74	50	13	48	77	24	370
$[PdPtMoCpCl(CO)_2(dppm)_2]$ (**3**)	−10.2	7.2 [c]	13.4 [c]	45.1	72	40	22.5	12	70	22	
$[Pd_2MoCp(CO)_3(dppm)_2][PF_6]$ [d] (**[4][PF$_6$]**)	−3.1	3.0	−9.0	44.4	55	27	26	38	69	7	
$[Pd_2WCp(CO)_3(dppm)_2][PF_6]$ [d] (**[5][PF$_6$]**)	−9.9	−1.5	−17.3	11.2	53	38	24	38	67	6	352
$[Pd_2WCpBr(CO)_2(dppm)_2]$ (**6**)	−17.5	−13.1	−11.0	17.2	76	50	14	48	76	15	380
$[Pd_2Mo_2Cp_2(CO)_5(dppm)_2]$ [e] (**9**)	−9.9	1.4	5.9	55.5	135.5	60	26	85.5	90	27	
$[Pd_2W_2Cp_2(CO)_5(dppm)_2]$ [e] (**10**)	−25.8	−8.3	−6.0	17.5	125	62	21	80	86	18	364
$[PdPtMo_2Cp_2(CO)_5(dppm)_2]$ [e] (**11**)	−12.9	14	21.3	50.6	117	44	34	23	75	24	

[a] Recorded in $CDCl_3/CH_2Cl_2$ (1/1) unless otherwise stated (δ in ppm; J in Hz). [b] Phosphorus assignment, see text for details. [c] ^{195}Pt satellites (^{1}J(PtP(2)) 3232, ^{1}J(PtP(3)) 3735 Hz). [d] The $[PF_6]^-$ anion exhibits a septuplet at −144 ppm (^{1}J(PF) 712 Hz). [e] Recorded in toluene with D_2O capillary lock. [f] ^{195}Pt satellites (^{1}J(PtP(2)) not determined, ^{1}J(PtP(3)) 3811 Hz).

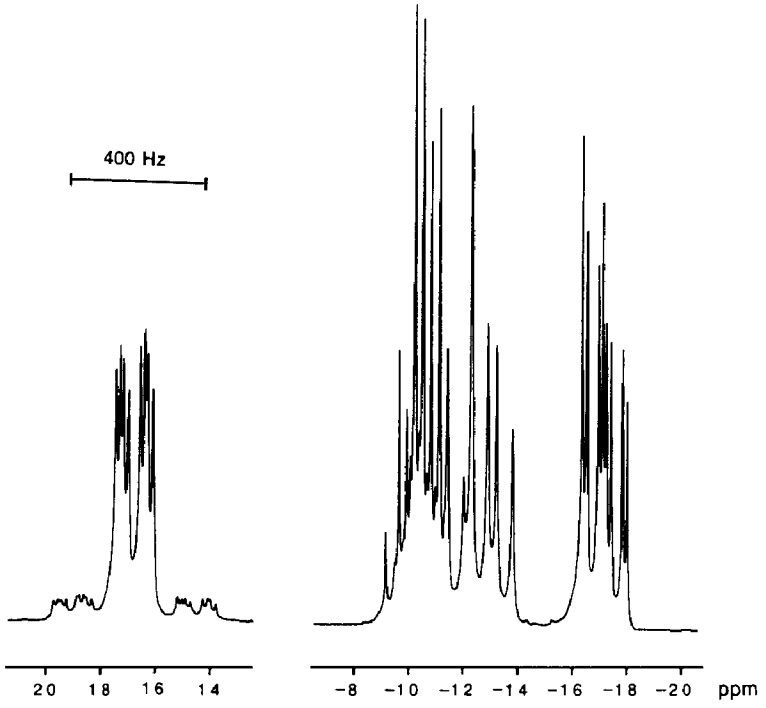

Fig. 1. $^{31}P\{^1H\}$ NMR spectrum of $[Pd_2WCpCl(CO)_2(\mu\text{-dppm})_2]$ (**2**).

Pd–Cl bond. This remains true even under conditions (room temperature, 2 equiv. carbonylmetalate) where other carbonylmetalates have led instead to metalloligated tetranuclear clusters [1]. Obviously, a Pd–Cl bond is preferred here to the formation of a $PdM(CO)_3Cp$ (M = Mo, W) unit. Although **1** or **2** were the only Pd–Mo(W) clusters isolated after work-up of the reaction mixture, we have strong evidence that they are not the primary products formed in the reaction of eq. 1. Thus, when a mixture of $[Pd_2Cl_2(\mu\text{-dppm})_2]$ and two equiv. of $Na[Mo(CO)_3Cp]$ was allowed to react at room temperature for 3 h, its $^{31}P\{^1H\}$ NMR and IR spectra revealed a mixture of **1**, $[\mathbf{4}]^+$, $[Mo(CO)_3Cp]^-$, $[Mo(CO)_3Cp]_2$ (low yield) and $[Pd_2Cl_2(\mu\text{-CO})(\mu\text{-dppm})_2]$ as the only observable products. Longer reaction times (2 d) only resulted in a small increase of the yield of $[Mo(CO)_3Cp]_2$, probably owing to slow oxidation (adventitious air) of the $[Mo(CO)_3Cp]^-$ anion. Similar observations were made with the Pd–W systems.

Bubbling CO through the reaction mixture increases the concentration of $[\mathbf{4}]^+$ (band at 2039 cm^{-1}), with no noticeable change in the other IR absorptions. This suggests that a precursor of $[\mathbf{4}]^+$, which could be $[\mathbf{7}]^+$, is also present at that time in the mixture, and could react according to eq. 4, as checked independently (for M = W).

$$[Pd_2MCp(CO)_2(THF)(\mu\text{-dppm})_2][M(CO)_3Cp] + CO \rightarrow$$

$$[\mathbf{7}]^+,\ M = Mo \qquad [Pd_2MCp(CO)_3(\mu\text{-dppm})_2][M(CO)_3Cp] \quad (4)$$

$$[\mathbf{8}]^+,\ M = W \qquad [\mathbf{4}]^+,\ M = Mo$$

$$[\mathbf{5}]^+,\ M = W$$

Similar carbonylation reactions of cationic solvento clusters with Pd_2Co or Pd_2Fe cores have been described previously [1e,f]. The anion associated with **[4]**$^+$ and **[7]**$^+$ is $[Mo(CO)_3Cp]^-$ and the strong ν(CO) bands at 1896 and ca. 1780 cm^{-1} are typical of the change of symmetry expected when this anion is associated with large cations [4]. That carbonylation of **[7]**$^+$ (**[8]**$^+$) by the CO released during the synthesis is facile is further supported by the relatively small amount of the A-frame complex $[Pd_2Cl_2(\mu\text{-CO})(\mu\text{-dppm})_2]$ [5] (2–7%) formed in competition (eq. 5).

$$[Pd_2Cl_2(\mu\text{-dppm})_2] + CO \rightarrow [Pd_2Cl_2(\mu\text{-CO})(\mu\text{-dppm})_2] \quad (5)$$

For comparison, this A-frame complex was found in 10–30% yield in the reactions of $[Pd_2Cl_2(\mu\text{-dppm})_2]$ with $[Co(CO)_4]^-$ or $[Fe(CO)_3NO]^-$, in which no other species was then competing with $[Pd_2Cl_2(\mu\text{-dppm})_2]$ for the CO released [1d–f].

Addition of chloride ions to the reaction mixture causes disappearance of the ν(CO) band at ca. 2040 cm^{-1} characteristic of **[4]**$^+$(**[5]**$^+$). This is consistent with the easy reaction of these cationic species (and a fortiori of **[7]**$^+$(**[8]**$^+$)) with Cl^- to give cluster **1** (**2**) (eq. 6) as independently verified by treating the $[PF_6]^-$ salts of these cations with LiCl in THF.

$$[Pd_2MCp(CO)_2L(\mu\text{-dppm})_2][M(CO)_3Cp] + Cl^- \xrightarrow{-L} [M(CO)_3Cp]^- + [Pd_2MCpCl(CO)_2(\mu\text{-dppm})_2] \quad (6)$$

[4]$^+$, M = Mo, L = CO

[5]$^+$, M = W, L = CO

[7]$^+$, M = Mo, L = THF

[8]$^+$, M = W, L = THF

1, M = Mo

2, M = W

This accounts for the formation of the latter clusters in eq. 1, as a result of the reaction of Cl^- (liberated during the synthesis) on the cationic species **[4]**$^+$(**[5]**$^+$) and **[7]**$^+$(**[8]**$^+$).

Following our observations on the role of the solvent on the formation or dissociation of metal–metal bonds [1c,6], the reaction mixture was evaporated and the solid dissolved in Et_2O. This solvent is less dissociating than THF, and should favour the formation of metal–metal bonds [7], i.e. of the exocyclic Pd–M bond in species such as **9** (**10**) (eq. 7).

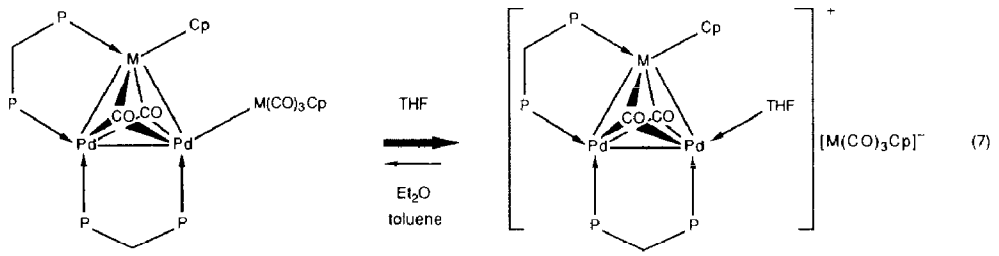

(7)

9, M = Mo

10, M = W

[7]$^+$, M = Mo

[8]$^+$, M = W

The Et_2O solution of the molybdenum-containing clusters was slightly green in colour, indicating formation of **9** (see below). Unfortunately, no product could be isolated because of rapid decomposition. In comparison, the reaction of $[Pd_2Cl_2(\mu\text{-dppm})_2]$ with two equiv of $[W(CO)_3Cp]^-$ had to be conducted in toluene instead of Et_2O in order to obtain a green solution indicative of **10** (see below) (eq. 8). Thus,

IR and $^{31}P\{^1H\}$ NMR spectra, recorded in toluene, are different from those of species such as **2**, $[5]^+$ or $[8]^+$, but rapid decomposition prevented isolation of pure **10**.

$$[Pd_2Cl_2(\mu\text{-dppm})_2] + 2[M(CO)_3Cp]^- \xrightarrow{Et_2O \text{ or toluene}}$$

$$M = Mo, W \qquad [Pd_2M_2Cp_2(CO)_5(\mu\text{-dppm})_2] + CO + 2Cl^- \qquad (8)$$

9, M = Mo;
10, M = W (not isolated)

Formation of the metalloligated clusters 9–11

In view of the difficulties encountered in the preparation of these clusters according to eq. 8, it was found to be advantageous to develop another route to these tetranuclear clusters. After reaching **1**, **2** or **3** with a slight excess of $[M(CO)_3Cp]^-$ in THF, the solvent was removed and extraction with toluene afforded the desired clusters **9**, **10** or **11**, respectively, in quantitative spectroscopic yields (eq. 9).

$$[PdM^1MCpCl(CO)_2(\mu\text{-dppm})_2] + [M(CO)_3Cp]^- \xrightarrow[2)\ \text{toluene}]{1)\ \text{THF}}$$

1, M^1 = Pd, M = Mo
2, M^1 = Pd, M = W
3, M^1 = Pt, M = Mo

$$[PdM^1M_2Cp_2(CO)_5(\mu\text{-dppm})_2] + Cl^- \qquad (9)$$

9, M^1 = Pd, M = Mo
10, M^1 = Pd, M = W
11, M^1 = Pt, M = Mo

The use of toluene in this reaction is essential for the in situ formation of the exocyclic Pd–M bond via collapse of the ion-pair complexes. The latter are regerenerated upon addition of THF to toluene solutions of the metalloligated clusters (eq. 7). Complete dissociation occurred upon addition of acetonitrile or CO or in pure THF.

It is now clear that the synthesis of **1** (**2**) from $[Pd_2Cl_2(\mu\text{-dppm})_2]$ occurs via the transient formation of **9** (**10**), which under the reaction conditions rapidly forms $[7]^+$($[8]^+$) (eq. 7), and this in turn reacts with the Cl^- present (eq. 6). In order to increase the rate of the chloride substitution reaction of eq. 6, the reaction mixture was heated to reflux. This also accelerates the decarbonylation of $[4]^+$ ($[5]^+$) and of the otherwise encountered byproduct $[Pd_2Cl_2(\mu\text{-CO})(\mu\text{-dppm})_2]$. Since the intermediates are thermally stable, quantitative conversion into **1** (**2**) is achieved. In contrast, when $[Pd_2Cl_2(\mu\text{-dppm})_2]$ was treated with one equiv of $[Fe(CO)_3NO]^-$ in refluxing THF, fragmentation occurred, to give homonuclear rather than mixed-metal products [3b].

*Crystal structure of $[Pd_2MoCpCl(CO)_2(\mu\text{-dppm})_2] \cdot 2C_6H_5Cl$ (**1** · 2PhCl)*

This cluster crystallizes with two molecules of chlorobenzene in the unit cell. There are no short contacts between the cluster and the PhCl molecules. Selected bond distances and angles are given in Table 4. The labelling scheme used in the description of the molecule on the ORTEP plot is shown in Figs. 2 and 3. The three metallic atoms form an almost equilateral triangle, as previously found for the tri- or tetranuclear dppm-bridged clusters $[Pd_2Co_2(CO)_7(\mu\text{-dppm})_2]$ [1a,d], $[Pd_2Co(CO)_4(\mu\text{-dppm})_2][PF_6]$ [1d] and $[Pd_2Mn_2(CO)_9(\mu\text{-dppm})_2]$ [1b,f]. The eight

Table 4

Selected interatomic distances (Å) and angles (°) in $[Pd_2MoCpCl(CO)_2(dppm)_2 \cdot 2C_6H_5Cl]$ (**1**·2PhCl) [a,b]

Pd(1)–Pd(2)	2.552(1)	Mo–Pd(1)–Pd(2)	62.8(1)
Pd(1)–Mo	2.779(1)	Pd(1)–Mo–Pd(2)	54.6(1)
Pd(2)–Mo	2.783(1)	Mo–Pd(2)–Pd(1)	62.6(1)
Pd(1)–P(1)	2.293(2)	Pd(2)–Pd(1)–P(1)	93.8(1)
Pd(2)–P(2)	2.300(2)	Pd(1)–Pd(2)–P(2)	97.5(1)
Pd(1)–P(3)	2.293(2)	Mo–Pd(1)–P(3)	100.9(1)
Mo–P(4)	2.481(2)	Pd(1)–Mo–P(4)	84.6(1)
Pd(2)–Cl	2.416(2)	P(1)–Pd(1)–P(3)	102.6(1)
Mo–Cp [c]	2.000(9)	Mo–Pd(2)–Cl	103.2(1)
Mo–C(1)	1.967(8)	P(2)–Pd(2)–Cl	96.7(1)
Mo–C(2)	1.985(9)	P(4)–Mo–Cp [c]	90.6(4)
Pd(1)–C(1)	2.478(8)	Mo–C(1)–O(1)	163.8(7)
Pd(1)–C(2)	2.389(9)	Mo–C(2)–O(2)	163.3(7)
Pd(2)–C(1)	2.512(8)	Mo–C(1)–Pd(1)	76.4(3)
Pd(2)–C(2)	2.544(8)	Mo–C(1)–Pd(2)	75.7(3)
		Mo–C(2)–Pd(1)	78.3(3)
		Mo–C(2)–Pd(2)	73.7(3)
		P(1)–C(3)–P(2)	108.7(4)
		P(3)–C(4)–P(4)	108.8(5)

[a] Atoms are labelled in agreement with Figs. 2 and 3. [b] Numbers in parentheses are estimated standard deviations in the last significant digit. [c] Centroid of the C_5H_5 ring.

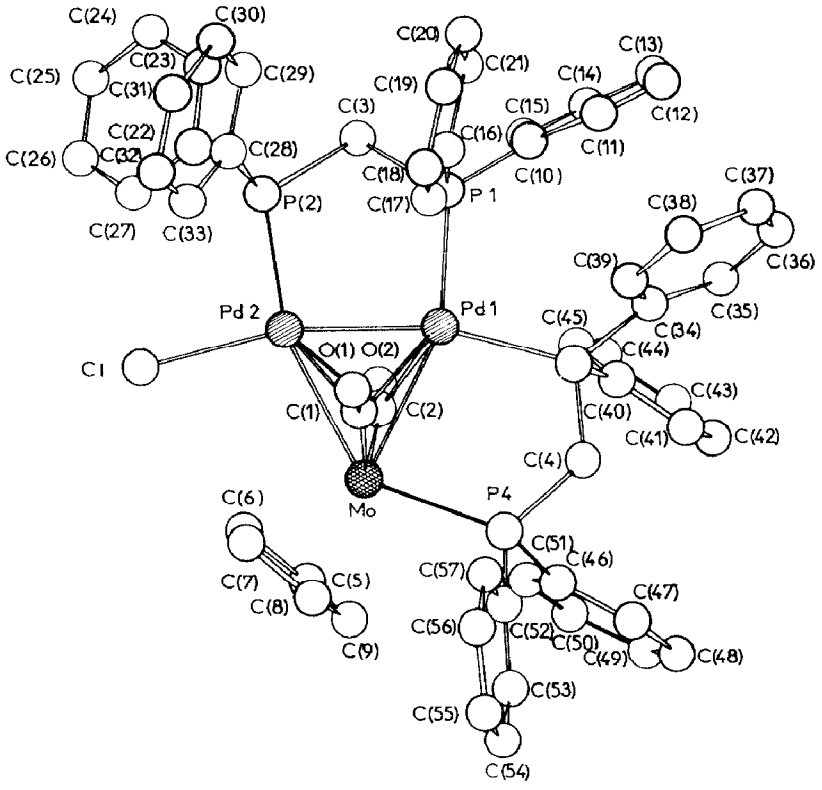

Fig. 2. Molecular structure of $[Pd_2MoCpCl(\mu\text{-}CO)_2(\mu\text{-}dppm)_2]$ (**1**) (top view) illustrating the atom numbering scheme. Thermal ellipsoids enclose 50% of the electron density.

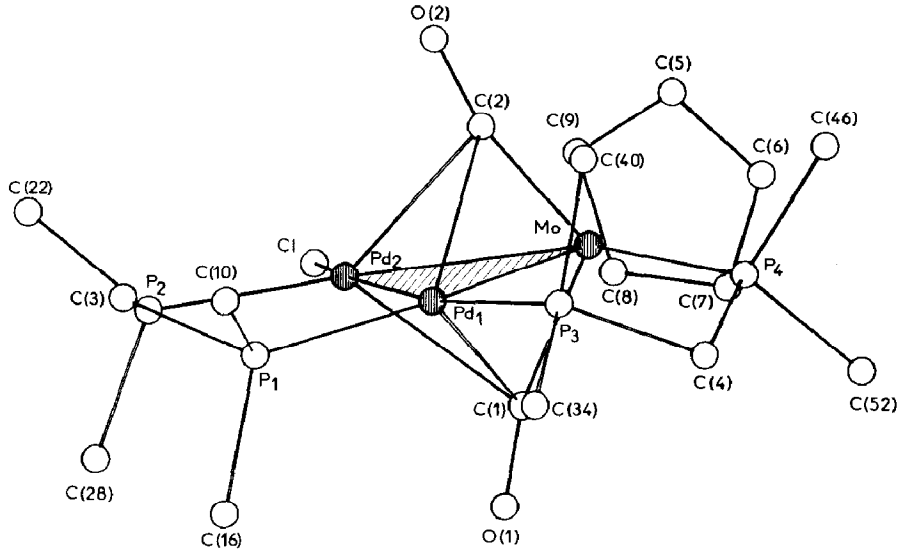

Fig. 3. Molecular structure of $[Pd_2MoCpCl(\mu\text{-}CO)_2(\mu\text{-}dppm)_2]$ (1) (perspective view). For clarity, the eight phenyl groups are represented by their *ipso* carbon atoms only.

atoms Pd(1), Pd(2), Mo, P(1), P(2), P(3), P(4), and Cl are almost coplanar. The four phosphorus atoms of the dppm ligands lie alternatively slightly above and below the trimetallic plane, the maximum deviation occurring for P(4) (0.311(2) Å). The Pd(1)–Pd(2) and Pd(1)–Mo bonds are each bridged by a dppm ligand. The Pd(1)–Pd(2) distance agrees well with that found in $[Pd_2Co(CO)_4(\mu\text{-}dppm)_2][PF_6]$, and appears to be slightly shorter than in the related tetranuclear clusters with Pd_2Co_2 or Pd_2Mn_2 cores. The two Pd–Mo bond lengths are in the range of those previously determined for Pd–Mo complexes [8]. The presence of a dppm bridge across the Pd(1)–Mo bond does not induce a significant shortening of this distance. The two carbonyl ligands are triply semibridging over the three metals, slightly closer to Pd(1) than to Pd(2), symmetrically arranged with respect to the metallic plane (distance from this plane to C(1): 1.794(9) Å and to C(2): −1.780(9) Å). These two carbonyl ligands are slightly bent (163.8(7), 163.3(7)°), and form with P(4) a "tripod" reminiscent of that in the $[Mo(CO)_3Cp]^-$ anion [9]. The angle between the cyclopentadienyl ring and the plane containing C(1), C(2), P(4) is 1.9°, while that with the trimetallic plane is 78.4°. The distance between Mo and the centroid of the Cp ring is 2.00 Å. These values are very close to those found in the planar, centrosymmetric cluster $[Pd_2Mo_2Cp_2(CO)_6(PEt_3)_2]$ [8].

The two carbon atoms C(3) and C(4) are on either side of the trimetallic plane. The Pd–P distances are similar whereas Mo–P(4) is longer. This could be due to the steric interaction between the cyclopentadienyl ligand and the phenyl groups at P(4) [10]. This constraint is further evidenced by the small value of the P(4)–Mo–Pd(1) angle (84.6(1)°) compared to the corresponding values in the other dppm bridge (93.8(1), 97.5(1)°). Furthermore, the angles between the planes of the two phenyls groups borne by each phosphorus atom fall in the range 108–117°, except at P(4) where the value is 135°. The chlorine atom is at a distance of 2.416 (2) Å from Pd(2) and 0.247 (3) Å away from the trimetallic plane. The angles Mo–Pd(2)–Cl (103.2(1)°) and Mo–Pd(1)–P(3) (100.9(1)°) are comparable.

Conclusion

The reaction of $[Pd_2Cl_2(\mu\text{-dppm})_2]$ with two equiv of $[M(CO)_3Cp]^-$ (M = Mo, W) in THF does not afford metalloligated tetranuclear clusters of the type previously seen with the anions $[Co(CO)_4]^-$, $[Fe(CO_3NO]^-$ or $[Mn(CO)_5]^-$ [1]. Instead, the clusters **1**, $[\mathbf{4}]^+$ (M = Mo) and **2**, $[\mathbf{5}]^+$ (M = W) are formed as the result of the ready reaction of Cl^- or CO with the cationic part of the intermediate $[Pd_2MCpL(CO)_2(\mu\text{-dppm})_2][M(CO)_3Cp]$ (M = Mo, W; L = THF). These considerations led us to optimize the synthesis of **1**, **2** or **3** by using only one equiv. of carbonylmetalate in refluxing THF. The metalloligated, tetranuclear cluster **9** or **10** appears to be formed only in poorly dissociating solvents such as Et_2O (for M = Mo) or toluene (for M = W). Both are very labile and decompose rapidly. Coordination of a bulky group at Pd(2) is prevented for steric reasons. Another example of a $Mo(CO)_3Cp$ fragment connected to a metallic triangle is found in the cluster $[Pt_2Mo_2Cp_2(CO)_6(dppe)]$ (dppe = $Ph_2PCH_2CH_2PPh_2$), where there is less crowding around the platinum atom bearing the exocyclic fragment [1a]. On the other hand, the stable tetranuclear metalloligated cluster $[Pd_2WCoCp(CO)_6(\mu\text{-dppm})_2]$, containing the less bulky $Co(CO)_4$ exocyclic fragment, has been isolated from the reaction of **2** with $[Co(CO)_4]^-$ [6].

The trinuclear clusters $[\mathbf{4}]^+$ and $[\mathbf{5}]^+$ belong to the very rare class of clusters having carbonyl ligand(s) terminally bound to palladium. Only two such examples, namely $[Pd_2Co(CO)_4(\mu\text{-dppm})_2][PF_6]$ [1d] and $[Pd_3Cl(CO)_2\{\mu\text{-P(t-Bu)}_2\}_3]$ [11], have been characterized, and those only recently, by X-ray diffraction studies. Clusters $[\mathbf{4}]^+$ and $[\mathbf{5}]^+$ display a reactivity somewhat different from that of structurally analogous clusters containing Pd_2Co or Pd_2Fe cores [1]. Thus for example, decarbonylation of $[\mathbf{4}]^+$ or $[\mathbf{5}]^+$ is not as easy, and formation of a tris-dppm-substituted cluster analogous to, e.g., $[Pd_2Co(CO)_2(\mu\text{-dppm})_3][PF_6]$ [1e] is hindered for steric reasons. The presence of a Pd–Cl bond in clusters **1**, **2** or **3** renders them attractive precursors for the synthesis of heterotetrametallic clusters by reaction with carbonylmetalate anions [1c,6].

Experimental

Reagents and physical measurements

All reactions were performed in Schlenk-type flasks under nitrogen. Tetrahydrofuran (THF), diethyl ether (Et_2O) and 1,2-dimethoxyethane (DME) were distilled under nitrogen from sodium benzophenone-ketyl prior to use. Chlorobenzene and dichloromethane were dried and distilled from P_2O_5. Toluene, n-hexane, and pentane were dried and distilled over sodium wire. Acetone was dried over $CaCl_2$. NMR deuterated solvents were degassed by three freeze-thaw cycles prior to use. Nitrogen was passed through a BASF R3-11 catalyst and molecular sieve columns to remove residual oxygen and water. Elemental analyses were performed by the Service Central de Microanalyses du CNRS. Infrared spectra were recorded in the region 4000–400 cm^{-1} on a Perkin–Elmer 398 spectrophotometer, and in the region 420–50 cm^{-1} on a Bruker IFS-113 interferometer as polyethylene disks, using 6 μm and 23 μm Mylar® beamsplitters. The ^1H and ^{31}P $\{^1H\}$ NMR spectra were recorded at 200.13 and 81.02 MHz respectively on a FT Bruker WP-200 SY instrument. The ^{13}C $\{^1H\}$ NMR spectra were recorded at 22.63 MHz on a FT

Bruker WH-90 instrument. Proton and carbon chemical shifts are positive downfield relative to external Me_4Si. Positive phosphorus chemical shifts indicate a downfield position relative to H_3PO_4.

Syntheses

$[Pd_2Cl_2(\mu\text{-dppm})_2]$ [5], $Na[Mo(CO)_3Cp]\cdot 2DME$ and $Na[W(CO)_3Cp]\cdot 2DME$ [8] were prepared as described previously. CO and other reagents were used as received.

Synthesis of $[Pd_2MoCpCl(CO)_2(\mu\text{-dppm})_2]$ (1). A mixture of $Na[Mo(CO)_3Cp]\cdot 2DME$ (0.506 g, 1.13 mmol, 13% excess) and $[Pd_2Cl_2(\mu\text{-dppm})_2]$ (1.05 g, 1.00 mmol) in THF (70 ml) was allowed to react at room temperature for 0.5 h after which a red precipitate of $[Pd_2Cl_2(\mu\text{-CO})(\mu\text{-dppm})_2]$ had formed. The mixture was then heated under reflux for 1 h, cooled and evaporated to dryness under reduced pressure. Extraction with CH_2Cl_2 (60 ml), filtration of the extract through a Celite-padded filter funnel, concentration to ca. 5 ml, and addition of n-hexane (40 ml) yielded green-brown crystals of **1** (1.03 g, 84% based on Pd) (m.p. 195 °C dec). Anal. Found: C, 51.88; H, 3.86; Cl, 3.89; Mo, 7.83; P, 10.15; Pd, 17.62. $C_{57}H_{49}ClMoO_2P_4Pd_2$ (M_r = 1234.14) calc: C, 55.47; H, 4.00; Cl, 2.87; Mo, 7.77; P, 10.04; Pd, 17.25%. FIR ν(PdCl) 258 cm^{-1}. $^{13}C\{^1H\}$ NMR (CD_2Cl_2) δ 212 (s, CO), 137–127 (m, Ph), 90.0 (s, Cp), 48.9 (m, CH_2), 51.4 (m, CH_2).

Synthesis of $[Pd_2WCpCl(CO)_2(\mu\text{-dppm})_2]$ (2). The procedure described for the synthesis of **1** was used, starting from $[Pd_2Cl_2(\mu\text{-dppm})_2]$ (2.17 g, 2.06 mmol) and $Na[W(CO)_3Cp]\cdot 2DME$ (1.11 g, 2.07 mmol). It afforded **2** as a green-brown powder after precipitation from the CH_2Cl_2 solution by addition of n-hexane (2.62 g, 1.98 mmol, 96% based on Pd). Slow diffusion of n-hexane (60 ml) into a CH_2Cl_2 (40 ml) solution of this powder yielded large dark crystals of **2** (1.74 g, 1.32 mmol, 64% based on Pd) (m.p. 194 °C dec). Anal. Found: C, 48.71; H, 3.70; Cl, 2.87; P, 9.38; Pd, 16.73; W, 14.46. $C_{57}H_{49}ClO_2P_4Pd_2W$ (M_r = 1322.05) calc: C, 51.78; H, 3.74; Cl, 2.68; P, 9.37; Pd, 16.10; W, 13.91%. FIR ν(PdCl) 257 cm^{-1}. $^{13}C\{^1H\}$ NMR CD_2Cl_2) δ 241 (s, CO), 136–127 (m, Ph), 87.7 (s, Cp), 48.9 (br, m, CH_2).

Synthesis of $[PdPtMoCpCl(CO)_2(\mu\text{-dppm})_2]$ (3). A procedure similar to that described for **1** was used, starting from $[PdPtCl_2(\mu\text{-dppm})_2]\cdot CH_2Cl_2$ (1.23 g, 1.00 mmol) and $Na[Mo(CO)_3Cp]\cdot 2DME$ (0.450 g, 1.00 mmol). Slow diffusion of n-hexane (70 ml) into the CH_2Cl_2 (20 ml) extract yielded large dark-red crystals of $3\cdot CH_2Cl_2$ (1.25 g, 0.89 mmol, 89% based on Pt). Anal. Found: C, 49.47; H, 3.68. $3\cdot CH_2Cl_2$ ($C_{58}H_{51}Cl_3MoO_2P_4PdPt$) ($M_r$ = 1407.73) calc: C, 49.49; H, 3.65%. FIR: ν(PdCl) 256 cm^{-1}.

Synthesis of $[Pd_2MoCp(CO)_3(\mu\text{-dppm})_2][PF_6]$ ([4][PF_6]). The following reaction and subsequent work-up procedures were performed under a CO atmosphere. A solution of $Tl[PF_6]$ (0.034 g, 0.10 mmol) in acetone (10 ml) was added to a solution of **1** (0.120 g, 0.10 mmol) in CH_2Cl_2 (100 ml), and CO was bubbled through the solution for 0.5 h. The color of the mixture slowly lightened. The mixture was then filtered through a Celite-padded filter funnel to remove insoluble TlCl. Addition of n-hexane to the filtrate gave a yellow-brown powder, which was recrystallized from CH_2Cl_2/n-hexane, affording **[4][PF_6]** as yellow-brown microcrystals (0.125 g, 90% based on Pd) (m.p. 178 °C dec.). Anal. Found: C, 47.04; H, 3.64. **[4][PF_6]**$\cdot 1.5CH_2Cl_2$ ($C_{59.5}H_{52}Cl_3F_6MoO_3P_5Pd_2$) ($M_r$ = 1499.06) calc: C, 47.67; H, 3.50%.

Synthesis of [$Pd_2WCp(CO)_3(\mu$-dppm)$_2$][PF_6]) ([5][PF_6]). The same procedure as described for the synthesis of [4][PF_6] was used, starting from **2** (0.392 g, 0.30 mmol) and Tl[PF_6] (0.112 g, 0.32 mmol). It afforded [5][PF_6] as orange-brown microcrystals (0.353 g, 82% based on Pd). Anal. Found: C, 48.37; H, 3.28. $C_{58}H_{49}F_6O_3P_5Pd_2W$ (M_r = 1459.57) calc: C, 47.73; H, 3.38%.

CO decoordination experiments. When a solution of [4][PF_6] in THF was evaporated to dryness in vacuo, its IR (KBr) spectrum was unchanged. Similar observations were made when THF was replaced by acetone or CH_2Cl_2. In contrast, when a solution of [4][PF_6] in MeCN was evaporated to dryness, the IR (KBr) spectrum of the solid showed bands due to [$Pd_2MoBrCp(CO)_2(\mu$-dppm)$_2$] (resulting from the solid-state reaction of the decarbonylated species with Br^-). Similar results were obtained starting from [5][PF_6].

Synthesis of [$Pd_2WCpBr(CO)_2(\mu$-dppm)$_2$] (6). Method A. A solution of **2** (0.236 g, 0.178 mmol) in acetone (50 ml) was stirred with NEt_4Br (0.210 g, a six-fold excess) for 3 h. The yellow-brown solution was filtered and n-hexane (100 ml) was added. The resulting powder was collected by filtration, washed with water (200 ml) to remove NEt_4Cl and NEt_4Br, and vacuum dried (0.207 g, 85% based on Pd) (m.p. 194 °C). Recrystallization from CH_2Cl_2/n-hexane afforded microcrystals of solvated **6**. Anal. Found: C, 47.86; H, 3.51. **6** · CH_2Cl_2 ($C_{58}H_{51}BrCl_2O_2P_4Pd_2W$) ($M_r$ = 1451.44) calc: C, 48.00; H, 3.54%.

Method B. Solid KBr (0.010 g, ca. threefold excess) was added to a solution of [5][PF_6] (0.050 g, 0.030 mmol) in acetone (10 ml). After 0.5 h stirring the acetone was evaporated off and the resulting solid was dissolved in CH_2Cl_2. The solution was filtered and n-hexane was added to precipitate **6** (0.037 g, 90% based on Pd).

Synthesis of [$Pd_2Mo_2Cp_2(CO)_5(\mu$-dppm)$_2$] (9). A brown solution of [$Pd_2MoCpCl(CO)_2$(dppm)$_2$] (0.296 g, 0.24 mmol) and Na[$Mo(CO)_3Cp$] · 2DME (0.135 g, 0.30 mmol, 20% excess) in THF (40 ml) was stirred for 0.5 h at 40 °C after which the solvent was removed. Addition of toluene (40 ml) caused a color change to deep emerald green. The solution was filtered through a Celite padded filter funnel and concentrated to ca. 20 ml. Slow evaporation of the solvent afforded microcrystals of unstable **9** (0.026 g; 0.018 mmol; 16% based on Pd). Anal. Found: C, 53.41; H, 4.01. $C_{65}H_{54}Mo_2O_5P_4Pd_2$ (M_r = 1443.76) calc: C, 54.07; H, 3.77%. All attempts (e.g., by cooling to −20 °C or by slow diffusion of n-hexane into a solution of **9**) to obtain X-ray quality crystals were unsuccessful, owing to the instability of this cluster.

Preparation and characterisation of [$Pd_2W_2Cp_2(CO)_5(\mu$-dppm)$_2$] (10) and [$PdPtMo_2Cp_2(CO)_5(\mu$-dppm)$_2$] (11). As noted for cluster **9**, these complexes cannot be stored for a long period of time. However, they can be prepared similarly, in quantitative yield, in solution (IR and $^{31}P\{^1H\}$ NMR evidence) for characterization and reactivity studies, but should be used immediately.

Attempted reaction of 2 with KO-t-Bu. Solid KO-t-Bu (0.018 g, 0.16 mmol) was added to a solution of **2** (0.218 g, 0.16 mmol) in THF (20 ml). After 1 h stirring solid NEt_4Cl (0.030 g, 0.18 mmol) was added in order to provide a large stabilizing cation. After stirring for 24 h, **2** was recovered (IR evidence).

Attempted reaction of 2 with MeLi. A solution of MeLi (1.55 *M* in Et_2O, 0.1 ml) was added from a syringe to a cooled solution (−78 °C) of **2** (0.203 g, 0.15 mmol) in THF (150 ml). No change of color occurred during stirring for 1 h. The temperature was then raised to ambient, and after overnight stirring the solution was evaporated to dryness. The resulting solid was washed with water and shown by analysis to be the pure **2** (IR and ^1H NMR spectroscopy).

Reaction of [5][PF_6] with MeLi (under CO). A solution of MeLi (1.55 *M* in Et_2O, 0.045 ml) was added from a syringe to a cooled solution (−78 °C) of [**5**][PF_6] (0.102 g, 0.07 mmol) in THF (20 ml) under a CO atmosphere. There was an immediate change of colour of the mixture from orange to deep red. The temperature was then raised to ambient with stirring. The red solution was evaporated to dryness and the IR (KBr) spectrum of the solid residue (in the ν(CO) region) showed bands at 1918m, 1872m and 1836vs cm^{-1}. The characteristic bands of $[\mathbf{5}]^+$ had completely disappeared. This residue was extracted with toluene (20 ml) to give a red solution and an insoluble orange-brown solid (0.060 g), characterized as [**5**][PF_6]. The ^{31}P {^1H} NMR spectrum of the toluene filtrate (in toluene-d_8) exhibited a singlet at 11 ppm, but no signal for $[PF_6]^-$.

Reaction of 2 with $HgCl_2$. Solid $HgCl_2$ (0.040 g, 0.15 mmol) was added to a solution of **2** (0.200 g, 0.15 mmol) in CH_2Cl_2 (50 ml). During 2 h stirring the

Table 5

Summary of crystal data and intensity collection of [$Pd_2MoCpCl(CO)_2(dppm)_2 \cdot 2C_6H_5Cl$] (**1**·2PhCl)

Formula	$C_{69}H_{59}Cl_3O_2MoP_4Pd_2$
FW	1458
crystal syst.	triclinic
space group	$P\bar{1}$-(C_i^1)
cryst. dimens. (mm)	0.1×0.2×0.2
a (Å)	13.664(2)
b (Å)	13.946(5)
c (Å)	18.223(6)
α (°)	110.30(3)
β (°)	93.89(2)
γ (°)	102.22(2)
V (Å^3)	3144.3(1)
Z	2
ρ (g/cm^3)	1.54
F(000) (e)	1468
temp. (°C)	20
diffractometer	Enraf–Nonius CAD 4 4F
radiation (graphite monochromator)	Mo-K_{α_1} (λ 0.70930 Å)
linear absorption coeff. (cm^{-1})	10.2
scan width (°)	1 + 0.35 tg θ
step width (°)	0.04
μ (aver. *R*)	$10.2 \times 2 \times 10^{-2}$
scan θ/scan ω	4/3
scan speed (°/s)	0.083
sin θ/λ_{max} (Å^{-1})	0.64
2θ limits (°)	2–27
octants collected	$\pm h, \pm k, l$
no. of data collected	9131
no. of unique data used	5675 ($I > 5\,\sigma(I)$)
$R = \Sigma \| \|F_0\| - \|F_c\| \| / \Sigma \|F_0\|$	0.046
$R_w = [\Sigma w(\|F_0\| - \|F_c\|)^2 / \Sigma w \|F_0\|^2]^{1/2}$	0.046
std. error in an observation of unit wt. (e)	1.2
largest shift/esd, final cycle	3.46
largest peak in final diff map (e/Å^3)	1.0

Table 6. Fractional coordinates ($\times 10^4$) and their estimated standard deviations for $[Pd_2MoCpCl(CO)_2(dppm)_2 \cdot 2C_6H_5Cl]$ (**1**·2PhCl)

Atom	*x*	*y*	*z*	*B* (Å^2) [a]
Pd(1)	995(1)	789(1)	2725(1)	2.46(2)
Pd(2)	2481(1)	246(1)	3253(1)	2.95(2)
Mo	558(1)	−1091(1)	2991(1)	2.50(2)
P(3)	−600(2)	869(2)	2314(2)	2.81(6)
P(1)	2007(2)	2249(2)	2606(2)	2.91(6)
P(2)	3738(2)	1684(2)	3336(2)	3.03(6)
P(4)	−1185(2)	−1312(2)	2360(2)	3.01(6)
Cl	3581(2)	−722(2)	3611(2)	4.98(7)
C(1)	1211(6)	−1020(6)	2075(5)	2.90(9)
O(1)	1529(6)	−1236(5)	1478(4)	4.66(9)
C(2)	863(6)	316(7)	3861(5)	3.38(9)
O(2)	969(5)	990(5)	4479(4)	4.42(9)
C(3)	3219(6)	2794(6)	3297(6)	3.73(9)
C(4)	−1370(7)	−488(6)	1773(6)	3.88(9)
C(5)	236(7)	−1890(7)	3939(7)	4.66(9)
C(6)	1291(7)	−1811(7)	3788(6)	4.02(9)
C(7)	1265(6)	−2451(6)	2983(6)	3.87(9)
C(8)	217(8)	−2920(6)	−2622(6)	4.66(9)
C(9)	−394(7)	−2551(7)	3223(7)	4.58(9)
C(10)	1513(6)	3423(7)	2853(6)	4.26(9)
C(11)	1082(8)	3730(7)	2279(7)	5.53(9)
C(12)	659(8)	4615(8)	2541(8)	6.95(10)
C(13)	696(9)	5171(8)	3328(7)	6.19(10)
C(14)	1092(8)	4867(8)	3901(7)	5.37(9)
C(15)	1511(8)	3979(7)	3655(7)	4.97(9)
C(16)	2417(6)	2070(7)	1649(6)	3.72(9)
C(17)	2295(8)	1056(8)	1104(6)	4.80(9)
C(18)	2639(8)	877(9)	365(7)	6.02(10)
C(19)	3086(8)	1750(9)	193(7)	6.62(10)
C(20)	3230(8)	2788(10)	746(8)	7.24(10)
C(21)	2901(8)	2960(8)	1478(7)	5.89(10)
C(22)	4695(6)	2320(7)	4229(5)	3.31(9)
C(23)	5204(7)	3454(7)	4402(7)	5.90(10)
C(24)	5891(8)	4016(8)	5115(7)	6.51(10)
C(25)	6067(8)	3529(8)	5631(7)	5.74(10)
C(26)	5580(8)	2500(9)	5453(7)	6.09(10)
C(27)	4875(7)	1923(8)	4747(6)	5.04(9)
C(28)	4496(6)	1407(7)	2529(5)	3.46(9)
C(29)	5004(8)	2198(9)	2297(7)	5.96(10)
C(30)	5557(9)	1966(9)	1687(8)	7.51(10)
C(31)	5623(8)	918(10)	1319(7)	6.56(10)
C(32)	5158(9)	152(8)	1570(7)	6.67(10)
C(33)	4568(7)	382(7)	2171(7)	5.06(9)
C(34)	−811(6)	1469(7)	1584(6)	3.47(9)
C(35)	−1377(7)	2220(8)	1716(6)	4.66(9)
C(36)	−1484(9)	2652(9)	1115(8)	7.05(10)
C(37)	−1051(9)	2314(9)	430(7)	6.58(10)
C(38)	−503(8)	1549(8)	315(7)	5.50(10)
C(39)	−375(7)	1141(7)	899(6)	4.06(9)
C(40)	−1257(6)	1467(7)	3120(5)	3.04(9)
C(41)	−2304(6)	1274(7)	3007(6)	4.12(9)
C(42)	−2743(8)	1764(8)	3668(8)	6.45(10)
C(43)	−2147(9)	2411(8)	4393(7)	6.41(10)

Table 6 (continued)

Atom	x	y	z	B (Å^2) [a]
C(44)	−1101(8)	2582(8)	4489(7)	5.39(10)
C(45)	−662(7)	2104(7)	3845(5)	3.52(9)
C(46)	−2199(6)	−1152(7)	2972(6)	3.63(9)
C(47)	−3205(6)	−1397(7)	2595(6)	4.42(9)
C(48)	−3960(7)	−1175(8)	3077(7)	4.97(9)
C(49)	−3724(7)	−751(8)	3888(7)	5.27(9)
C(50)	−2707(8)	−537(8)	4256(6)	4.87(9)
C(51)	−1945(7)	−744(7)	3782(6)	3.83(9)
C(52)	−1663(8)	7363(7)	1587(7)	5.17(9)
C(53)	−2387(7)	6576(7)	1699(7)	5.59(10)
C(54)	−2644(9)	5550(9)	1105(9)	8.60(10)
C(55)	−2164(10)	5339(9)	444(9)	8.69(10)
C(56)	−1425(10)	6117(9)	318(8)	8.34(10)
C(57)	−1168(8)	7134(8)	905(6)	5.96(10)
Cl(2)	4537(5)	5054(5)	7449(5)	15.83(9)
C(58)	3469(9)	4579(10)	6741(8)	7.68(13)
C(59)	2873(9)	5248(9)	6771(8)	9.24(10)
C(60)	1977(11)	4889(12)	6175(10)	14.23(10)
C(61)	1790(10)	3823(13)	5629(9)	13.88(10)
C(62)	2482(11)	3261(11)	5638(9)	13.42(10)
C(63)	3300(10)	3546(10)	6168(9)	9.89(10)
Cl(3)	6701(6)	3902(5)	7806(4)	16.98(9)
C(64)	6216(10)	3355(11)	8477(8)	9.48(10)
C(65)	5474(9)	3807(10)	8846(9)	9.13(10)
C(66)	5202(10)	3489(11)	9458(10)	10.50(10)
C(67)	5686(11)	2787(11)	9747(10)	12.05(10)
C(68)	6405(10)	2419(10)	9250(9)	10.40(10)
C(69)	6711(10)	2684(10)	8648(8)	8.29(13)

[a] Anisotropically refined atoms are given in the form of the isotropic equivalent thermal parameters: B (Å^2) $= (4/3)[\beta_{11}a^2 + \beta_{22}b^2 + \beta_{33}c^2 + \beta_{12}ab\cos\gamma + \beta_{13}ac\cos\beta + \beta_{23}bc\cos\alpha]$.

mixture turned slowly from yellow-brown to green-brown and eventually to dark brown. The solvent was evaporated off, and the IR (KBr) spectrum of the solid residue showed the characteristic bands of dppm but no absorption in the ν(CO) region. The solid was extracted with CH_2Cl_2, affording a yellow solution and leaving some black insoluble material. The solution was shown by $^{31}P\{^1H\}$ and ^1H NMR spectroscopy to contain mainly $[PdCl_2(dppm)]$ [12] (some peaks appeared in the 20–40 ppm region of the $^{31}P\{^1H\}$ NMR spectrum, but were not attributed to Hg-dppm complexes, due to the lack of ^{199}Hg satellites).

Reaction of $[Pd_2Cl_2(\mu\text{-dppm})_2]$ with $HgCl_2$. Solid $HgCl_2$ (0.003 g, 0.011 mmol) was added to a solution of $[Pd_2Cl_2(\mu\text{-dppm})_2]$ (0.020 g, 0.019 mmol) in 1 ml of a mixture of CH_2Cl_2 and $CDCl_3$. Upon stirring, the solution turned from orange to pale yellow within 5 min. The solution was filtered and transferred to a NMR tube. The $^{31}P\{^1H\}$ spectrum exhibited a singlet at −54.1 ppm, attributed to $[PdCl_2(dppm)]$ and a weaker peak at 9.6 ppm.

X-ray data collection and structure determination of $\mathbf{1}\cdot 2C_6H_5Cl$

Single crystals of **1** were obtained by dissolving the complex in a mixture of CH_2Cl_2 (50 ml) and PhCl (50 ml), followed by evaporation of the CH_2Cl_2 under

reduced pressure and addition of a layer of n-hexane to the residual solution. Crystal data, cell constants and other pertinent data are presented in Table 5.

The structure was solved by Patterson method for Pd and Mo atoms and by Fourier syntheses for C, O, P and Cl atoms. Refinements have been carried out by full-matrix least squares (all non-hydrogen atoms anisotropic) using the SHELX program [13]. The atomic scattering factors used, corrected for the anomalous dispersion of the metal atoms, were taken from the literature [14]. Final positional parameters are given in Table 6.

Anisotropic thermal parameters, observed and calculated structure factor amplitudes of the reflections used in the refinement are available as supplementary material [15].

Acknowledgment

We are grateful to the CNRS for financial support and for a grant to M. R., and we also thank the Johnson Matthey Technology Center for a generous loan of $PdCl_2$.

Supplementary Material Available

Tables of complete bond lengths and angles and a table of selected weighted least-squares planes have been deposited at the Cambridge Crystallographic Data Centre. Tables of thermal parameters and observed and calculated structure factors are available from the authors.

References

1 (a) P. Braunstein, J.-M. Jud, Y. Dusausoy and J. Fischer, Organometallics, 2 (1983) 180; (b) P. Braunstein, J.-M. Jud and J. Fischer, J. Chem. Soc., Chem. Commun., (1983) 5; (c) P. Braunstein, C. de Méric de Bellefon and M. Ries, J. Organomet. Chem., 262 (1984) C14; (d) P. Braunstein, C. de Méric de Bellefon, M. Ries, J. Fischer, S.E. Bouaoud and D. Grandjean, Inorg. Chem., 27 (1988) 1327; (e) P. Braunstein, C. de Méric de Bellefon and M. Ries, Inorg. Chem., 27 (1988) 1338; (f) P. Braunstein, C. de Méric de Bellefon, M. Ries and J. Fischer, Organometallics, 7 (1988) 332.
2 See, for example: S. Al Jibori and B.L. Shaw, Inorg. Chim. Acta, 74 (1983) 235.
3 (a) P. Braunstein, J. Kervennal and J.-L. Richert, Angew. Chem. Int. Ed. Engl., 24 (1985) 768; (b) P. Braunstein and J.-L. Richert, unpublished results.
4 M.Y. Darensbourg, P. Jimenez, J.R. Sackett, J.M. Hanckel and R.L. Kump, J. Am. Chem. Soc. 104 (1982) 1521.
5 L.S. Benner and A.L. Balch, J. Am. Chem. Soc., 100 (1978) 6099.
6 (a) M. Ries, Doctorat Thesis, Université Louis Pasteur, Strasbourg, September 1987; (b) P. Braunstein, C. de Méric de Bellefon and M. Ries, manuscript in preparation.
7 E.O. Fischer, T.L. Linder, F.R. Kreissl and P. Braunstein, Chem. Ber., 110 (1977) 3139.
8 R. Bender, P. Braunstein J.-M. Jud and Y. Dusausoy, Inorg. Chem., 22 (1983) 3394.
9 D.E. Crotty, E.R. Corey, T.J. Anderson, M.D. Glick and J.P. Oliver, Inorg. Chem., 16 (1977) 920.
10 R. Bender, P. Braunstein and C. de Méric de Bellefon, Polyhedron, (1988) in press.
11 A.M. Arif, D.E. Heaton, R.A. Jones and C.M. Nunn, Inorg. Chem. 26 (1987) 4228.
12 C.T. Hunt and A.L. Balch, Inorg. Chem., 20 (1981) 2267.
13 G.M. Sheldrick, SHELX, System of Crystallographic Computer Programs, University of Cambridge, 1976.
14 International Tables for X-Ray Crystallography, Kynoch Press, Birmingham, England 1974, IV.
15 See paragraph at the end of the paper regarding supplementary material.